



Experimental and Numerical Simulation of Thermal Storage Capsule in AC Duct System

Hussein A. Al-Kutuby¹ and Maathe A. Theeb¹

Affiliations

¹ Mechanical Engineering Department, College of Engineering, University of Mustansiriyah, Baghdad, Iraq

Correspondence

Prof.Dr.Maathe A.Theeb
maathe@uomustansiriya.edu.iq

Received

22-September-2023

Revised

01-October-2023

Accepted

28-November-2023

Doi 10.31185/ejuow.Vol11.Iss3.485

Abstract

This experimental and numerical study investigates the effect of porous media on the thermal storage behaviour of a refrigeration duct system. The study presents the transient behaviour of heat absorption and Nusselt number for different velocities and porous media presence/absence cases. Results show that the heat transfer rate decreases over time, with the presence of porous media, providing resistance to heat absorption, particularly at relatively low velocities. The Nusselt number decreases slightly over time, but it increases as the velocity increases in all cases, with the maximum value observed at a velocity of 3 m/s. The presence of porous media significantly enhances heat transfer, with an improvement of up to 150% at a lower velocity of 1.5 m/s and 110% at an inlet velocity of 2.25 m/s. The study provides a comprehensive visualisation of the heat transfer process through contour analysis of temperature distribution, allowing better understanding of the thermal storage system's design and performance. The findings have implications for the optimisation of thermal storage systems in various applications, including energy-efficient buildings and renewable energy systems.

Keywords: thermal storage, phase change material, porous media, Nusselt number, contour analysis.

الخلاصة: تبحت هذه الدراسة التجريبية والعديدية في تأثير الوسائط المسامية على سلوك التخزين الحراري لنظام قنوات التبريد. قدمت الدراسة السلوك العابر لامتصاص الحرارة ورقم نسلت للسرعات المختلفة وحالات وجود/غياب الوسائط المسامية. أظهرت النتائج أن معدل انتقال الحرارة يتناقص بمرور الوقت، مع وجود وسائط مسامية، مما يوفر مقاومة لامتصاص الحرارة، خاصة عند السرعات المنخفضة نسبيًا. يتناقص عدد نسلت قليلاً مع مرور الوقت، لكنه يزداد مع زيادة السرعة في جميع الحالات، مع ملاحظة القيمة القصوى عند سرعة 3 م/ث. يؤدي وجود الوسائط المسامية إلى تعزيز انتقال الحرارة بشكل كبير، مع تحسن يصل إلى 150% عند سرعة أقل تبلغ 1.5 م/ث و110% عند سرعة مدخل تبلغ 2.25 م/ث. توفر الدراسة تصورًا شاملاً لعملية نقل الحرارة من خلال التحليل الكفافي لتوزيع درجة الحرارة، مما يسمح بفهم أفضل لتصميم وأداء نظام التخزين الحراري. النتائج لها آثار على تحسين أنظمة التخزين الحراري في مختلف التطبيقات، بما في ذلك المباني الموفرة للطاقة وأنظمة الطاقة المتجددة.

1. Introduction

Energy efficiency has emerged as a pressing issue, at present, with the rising global demand for energy and the dwindling supply of fossil fuels. As a result, the use of renewable energy sources is crucial, and solar power is effective due to its many advantages (such as renewability, abundance, accessibility and lack of pollution). Latent thermal energy preservation involves a phase shift at a fixed temperature, whereas thermochemical and perceptible thermal energy storage uses other processes. A material's chemical and thermal stability at high temperatures is essential for any sensible thermal energy storage (STES) system. Thermochemical energy storage (TCES) devices can temporarily store and recover heat through chemical processes, but they have limited useful lives and require certain conditions to function. Evidence indicates that latent thermal energy storage (LTESS) devices based on phase change materials (PCM) may store considerable heat at low working temperatures [1]. PCMs can store sensible and latent heat; thus, they may be used for heating and cooling. Low-temperature energy storage is used in various applications, including solar air collectors [2], thermal energy storage of structural components and refrigeration [4], drying techniques and construction equipment, such as domestic hot water [5], cold storage and waste heat recovery systems. PCMs alter their crystalline structure during the solid–solid phase transition, resulting in thermal energy storage. However, at a slow pace and with a low energy storage density [6], they are more feasible than gas phase change systems. Solid–liquid transition PCMS are popular due to their low

volume change, mobility, high thermal energy density and compact size [7]. Despite that a solid–liquid transition is found in the vast majority of materials, many materials lack the qualities essential for practical applications [8, 9].

In molecular concept, paraffins (waxes) are represented by the formula $C_n H_{(2n+2)}$ because they are a byproduct of the refining process. Paraffin may be used at low temperatures because its phase transition temperature is between 18 °C and 71 °C [10]. Low manufacturing costs allow its widespread use, significantly reducing the price of the product compared with using pure n-alkanes. Paraffins have a number of benefits, including high latent heat density, low vapour pressure, lack of phase separation and self-nucleation. Fluidity issues, incompatibility with containers and poor heat conductivity [11] cause problematic usage of paraffins. Methods for boosting heat transmission might lead to greater thermal conductivity. Improvements include new shapes and sizes for the shell, heat-transferring fins, numerous tubes, the use of nano-particles in PCMs and other innovations. These methods may be analysed computationally and experimentally (theoretically). Fatty acids, which have the formula $CH_3(CH_2)_nCOOH$, are carboxylic acids consisting of long chains of hydrocarbons. A eutectic mixture of two or more fatty acids has several advantages. [12] In a temperature window of approximately 16 °C to 74 °C, a phase change may take place.

Natural convection is a major aid in PCM melting. The buoyancy forces create vortices in the flow, which speeds up the heat transfer rate. The direction in which the surface heat is moving affects the melting time of PCMs and the rate of spontaneous convection. PCMs are ineffective heat transfer media due to their poor heat transmission properties. Heat conduction in PCM-based thermal energy storage devices should be improved to be utilized. Extra HTF tubes are integrated inside the power conversion module to improve the shell and tube LTESS's subpar thermal performance. Agyenim et al. [13] used erythritol as a PCM to evaluate the effectiveness of a horizontal shell and tube heat exchanger in storing thermal energy. The degree of temperature maintenance discrepancy between the tube and shell systems was measured. A 3.5 percentage point increase was found in the axial and radial phase shifts. Esapour et al. [14] conducted an empirical investigation of melting in a multi-tube heat exchanger. Shortening PCM melting time by 29% is achieved with single-tube splitting. Figure 2.1 shows how the results shift when the heat transfer tube temperature changes (b). For all configurations, melting times decreased by 33% when the HTF input temperature was raised from 50 °C to 60 °C. Liu et al. [15] used several configurations of big and small HTF tubes to quantify the melting process of RT27 (paraffin mix) as a PCM. The number of tubes used and the diameter ratio of the tubes might have a role on the heat transfer pace. PCM melting was hastened by joining a large tube to two smaller tubes with a 2:1 diameter ratio. Liu et al. [16] used paraffin as the PCM and air as the HTF in their LTESS numerical simulations. The melting rate and the convective heat transfer are increased by 57% when staggered tubes are used. Paraffin wax melting in a horizontal double-pipe heat storage system was studied by Jesumathy et al. [17]. They investigated the effect of HTF temperature and mass flow rates. When the input temperature to the HTF was raised by 2 °C, the melting rate rose by 25%. Kousha et al. [18] studied the melting and solidification of finless multi-tube heat exchangers at different HTF temperatures. Paraffin (RT-35) was used as PCM, and it was stored in cylindrical containers. The melting and solidification periods were reduced by 43% and 50%, respectively, using four HTF tubes. In their study, Joybari et al. [19] compared the performance of single and multiple (five tubes) finless vertical heat exchangers in the melting of paraffin (RT-60). The PCM melting process was sped up because of the enhanced convective effects of the multi-tube design. The melting time was reduced by 72.4% because of the multiple tube configuration. Multi-tube LTESS experiments have been conducted earlier, but their vast majority ignored fins. Fins and HTF configurations with multiple tubes may speed up the melting process. Variable-sized and shaped fins added to LTESS improve its performance [19-23]. For better heat conduction, Yousef et al. [24] used a PCM-based solar still on hollowed pin-type fins. Here, we compared pin finned systems built with PCM technology to those built without PCM technology and to conventional PCM-based systems. Charging and discharging of PCMs are enhanced by longitudinal fins rather than circular ones [25, 26]. Several investigations have examined how the presence of longitudinal fins [27], fin positions [28] and shell form [29] influence PCM melting. PCMs melted rapidly because the blades were large, long, and numerous. PCM paraffin RT35 melting in a vertical LTESS with circular fins was studied by Yang et al. [30]. The researchers confirmed whether more annular fins surrounding an HTF tube might have a different impact on PCM melting. The 31 annular fins on the LTESS allowed the fastest melting time. Extensive studies on the effect of thermo-physical and geometric factors on the efficiency of horizontal sleeve–tube LTESS were conducted by Wang et al. [31]. The melting of polycrystalline methanol (PCM) was examined to see how factors, such as fin height, shape, slope among fins and conducting shells, affected the process. The PCM melting time was reduced by 49.1%.

PCMs have been proposed as a potential solution to improve the energy efficiency of refrigeration systems. Several studies have investigated the use of PCMs in refrigeration systems for various applications. In this literature review, we summarise some of the recent studies that have investigated the use of PCMs in refrigeration systems. One study by Khodabandeh et al. [32] investigated the use of paraffin wax as a PCM in a domestic

refrigerator. The study found that the use of the PCM reduced the compressor run time by up to 50%, leading to a 28% reduction in energy consumption. Another study by Wang et al. [33] investigated the use of a eutectic mixture of capric acid and lauric acid as a PCM in a refrigeration system for food preservation. The study found that the use of PCM reduced the temperature fluctuations in the refrigeration compartment and improved the overall energy efficiency of the system. Zhang et al. [34] proposed a novel refrigeration system that used a PCM-based thermal storage unit for cooling. The system consisted of a refrigeration cycle, a PCM-based thermal storage unit and a heat exchanger. The study found that the use of the PCM-based thermal storage unit reduced the compressor run time and improved the overall energy efficiency of the system. In a study by Zhu et al. [35], a hybrid refrigeration system that combined a vapor compression cycle with a PCM-based thermal storage unit was proposed. The study found that the use of the PCM-based thermal storage unit improved the energy efficiency of the system and reduced the compressor run time. Another study by Zhang et al. [36] investigated the use of a PCM-based thermal storage unit in a supermarket refrigeration system. The study found that the use of the PCM-based thermal storage unit reduced the peak energy demand and improved the energy efficiency of the system. Overall, these studies suggest that the use of PCMs in refrigeration systems can improve the energy efficiency of the system and reduce the energy consumption. However, further research is required to optimise the design of PCM-based refrigeration systems for various applications.

1.1 Aim of the work

This work is devoted to studying the thermal behaviour of PCM with and without metal foam (MF). A capsulated cylinder is subjected to hot air at different temperatures and the aim is to measure the total melting time under different conditions. The aims can be listed as:

- The total melting time measuring of PCM with and without MF experimentally and comparing the result with theoretical data.
- Study the influence of changing the air temperature that passes through the insulated duct where the copulated cylinder is located.
- Study the influence of increasing the insulation thickness of the MF that the air is passed through and subsequently on the melting duration time of the PCM.
- Optimize the studied parameters to decrease the time of charging.

2. Methodology

2.1 Experimental Work

The prototype has a piece for the capsule that is one meter long, as shown in Figure (1). The setup consists of a copper pipe with a diameter of 2 inches and a length of 30 cm, containing a PCM called wax. A metal foam is added around the pipe (wrapping the pipe) to improve the PCM's thermal conductivity. The entrance duct is made of galvanised iron with a thickness of 1.5 mm and insulated with black foam to prevent heat losses from the system. The duct has a heater of 1000 watts, which will pre-heat air facing the copper pipe that contains the PCM, a blower with a centrifugal fan and a fan at the end for discharging. The blower section is connected to the entry section through a transition section made of galvanised steel and PVC pipes. The Reynolds number of the turbulent flow ranges from 2752.93 to 27529.25, and wire mesh is used to reduce incoming air disturbance. Three 1 mm thick Perspex sheets and one 1 mm thick nylon sheet were used to enclose the setup. The air ducts and the sealed area have a cross-section of 100 mm by 25 mm. The waste air is released into the environment, and only the top and bottom surfaces of the test section allow airflow. The components are secured together using chloroform acrylic glue and QS-5000 super-strong cyanoacrylate adhesive. The thermophysical characteristics of PCM and copper are summarised together with other metals in the following table (Table 1).

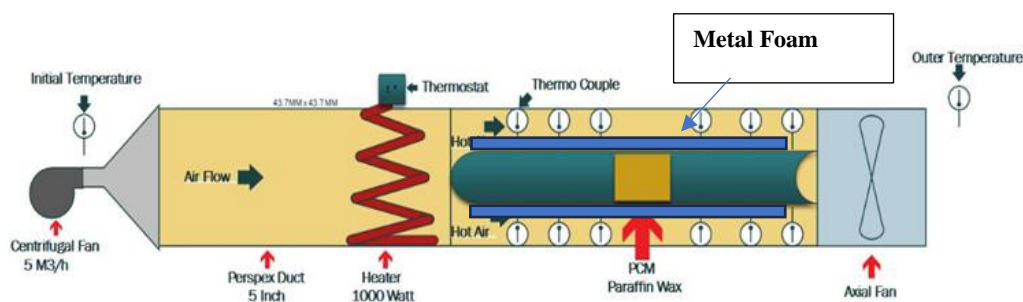


Figure (1) Experimental rig setup.

Table (1) Thermophysical properties of PCM and Copper.

Property	PCM	Copper
Density of PCM, Solid, $\rho_s(kg/m^3)$	930	8978
Density of PCM, Liquid, $\rho_l(kg/m^3)$	830	–
Specific heat of PCM, $c_{Ps}, c_{Pl}(J/kg\cdot K)$	2100	381
Thermal conductivity (w/m.K)	0.21	387.6
Melting temperature, T (°C)	48	–
Dynamic viscosity $\mu (kg/m\cdot s)$	0.03499	–
Latent heat of fusion, L (J/kg)	190000	–
Thermal expansion (1/K)	0.00011	–

To conduct experiments on the discharge process of the STES system, the following method was used:

1. Three test section boxes were filled with liquid PCM2 and allowed to cool down. PCM was poured into the copper pipe of the test section, and a sight glass in the pipe's centre is used to monitor the melting process.
2. The PCM was melted using electrical box heaters whilst ensuring appropriate insulation of all duct devices.
3. Thermocouples were used to examine temperature distribution, and the fan was turned on at different velocities (1.5, 2.25, and 3 m/s) for the basic and enhanced cases.
4. The heaters were shut off when the temperature at the box's base had risen to several degrees Celsius above the melting point of PCM, and the heater was turned on until a fixed temperature inlet (60 °C, 65 °C, and 70 °C) is reached for the basic and enhanced cases.

5. Time was allowed to pass to verify that the PCM temperatures reached approximately 70 °C and were distributed uniformly throughout all boxes, with data saved every 30 minutes.
6. The fan was activated at a predetermined speed.
7. A temperature recorder was used to log temperatures read from the thermocouples every 30 seconds.
8. The process was continued until the PCM in all containers reached 50 °C; the data were saved to find the better case that consumed less time in melting.
9. The same steps were repeated with the four remaining velocities. Similar experiments were conducted on the CTES and MF-CTES systems, with different PCMs and metal foam porosities used.

2.2 Numerical Simulation

Surplus heat is collected from an air conditioner to be used for heating the domestic water or storing it for any heating purposes to achieve the objective of using PCM capsules as a thermal storage. PCM and other materials are a promising solution for this case. They are used to store heat because they have the required heat fusion to store heat as much as possible. Numerical research into the equations of conservation of mass, momentum and energy is performed using CFD computer simulation to undertake a numerical study of this system (Fluent 2021 R1). To some extent, the program may help you estimate how well the design works. This chapter provides the reader a detailed breakdown of the parametric research and the computational approach. A rectangular duct, 10 cm wide by 10 cm tall, is used in the heat recovery process of the cooling system, as illustrated in Figure (2). The PCM capsule, which is a thermal energy storage device, is 30 cm tall and 5 cm in diameter. A typical copper pipe has a 2-mm wall thickness. Prior to sealing, the PCM-filled capsule was used to store heat (paraffin wax). The hot air was carried via the duct and transferred heat from the flow streaming site to the capsule system, which serves as the thermal storage.

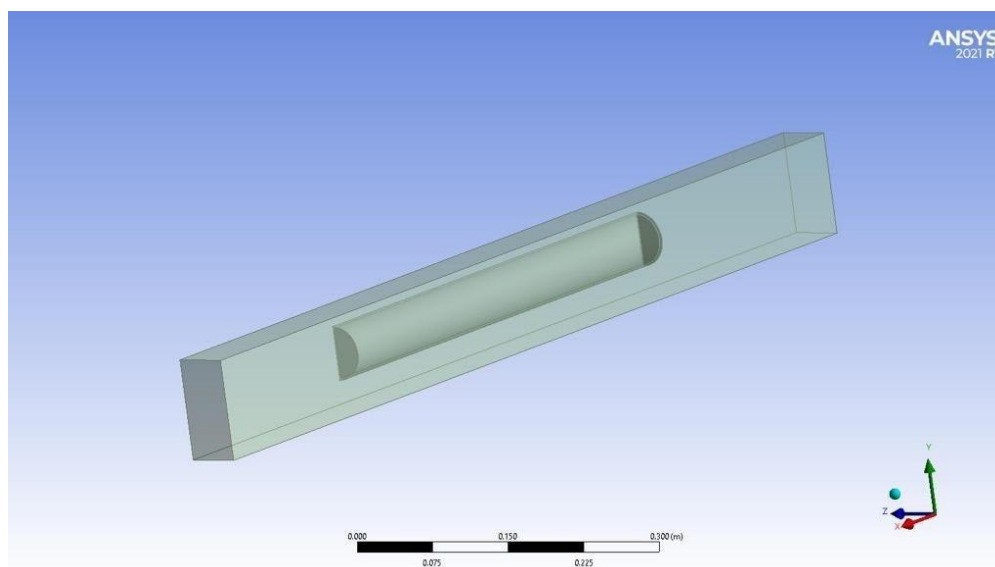


Figure (2): Thermal energy storage geometry.

We simulated the thermal storage waste heat system in the software Fluent 2021 R1 to reliably predict the solidification and melting processes of the PCM. The programme was useful in achieving these objectives. Solid Work was used to produce the cylinder tube and the Cartesian tube in all three dimensions (x, y and Z), and the Gambit software was used to mesh the geometry of the cylinder tube. After the creation of zones and boundary layers, the mesh was sent to the fluent program for further processing. Figure 2 depicts the stages of a typical numerical analysis.

The governing equations of conservation are as follows:

2.2.1 Continuity equation

$$\frac{\partial \rho_f}{\partial t} = - \left[\frac{\partial(\rho_f U)}{\partial x} + \frac{\partial(\rho_f V)}{\partial y} + \frac{\partial(\rho_f W)}{\partial z} \right] \quad (1)$$

2.2.2 Momentum equation

The enthalpy–porosity technique considers the mushy region as partially solidified, such as a porous media. Thus, porosity in each cell is set equal to the LF on the cell. The following form is considered a momentum sink due to the reduction of the porosity in the mushy zone, as follows:

$$S = \frac{(1-\text{vol})^2}{(\text{vol}^3+n)} A \vec{V}_f \vec{V}_{Pf} \quad (2)$$

where vol=liquid volume fraction.

n =constant small number (0.001) to prevent division by zero.

\vec{V}_{Pf} = velocity of the solid substance when being pulled out of the region.

A = constant value of mush region.

The main transport equations when using ANSYS Fluent 16 in the present work are as follows [20]:

$$\rho_f \frac{dU}{dt} + \rho_f \left[U \frac{\partial(U)}{\partial x} + V \frac{\partial(U)}{\partial y} + W \frac{\partial(U)}{\partial z} \right] = \mu \left[\frac{\partial^2(U)}{\partial x^2} + \frac{\partial^2(U)}{\partial y^2} + \frac{\partial^2(U)}{\partial z^2} \right] + \rho_f g \quad (3a)$$

$$\rho_f \frac{dV}{dt} + \rho_f \left[U \frac{\partial(V)}{\partial x} + V \frac{\partial(V)}{\partial y} + W \frac{\partial(V)}{\partial z} \right] = \mu \left[\frac{\partial^2(V)}{\partial x^2} + \frac{\partial^2(V)}{\partial y^2} + \frac{\partial^2(V)}{\partial z^2} \right] + \rho_f g \quad (3b)$$

$$\rho_f \frac{dW}{dt} + \rho_f \left[U \frac{\partial(W)}{\partial x} + V \frac{\partial(W)}{\partial y} + W \frac{\partial(W)}{\partial z} \right] = \mu \left[\frac{\partial^2(W)}{\partial x^2} + \frac{\partial^2(W)}{\partial y^2} + \frac{\partial^2(W)}{\partial z^2} \right] + \rho_f g \quad (3c)$$

where μ is the dynamic viscosity, ρ is density, and U is used velocity. The continuity equation (3) consists of the conservation of control volume mass with inflow and outflow transported mass. Navier–Stoke equations refer to the equality of inertia term to the sum of viscous force and gravity force.

2.2.3 Energy equation

The total sensible heat, h_f , and the latent heat, H_f , are calculated as follows: The following equation describes a material's enthalpy:

$$H_f = h_f + \Delta H_f \quad (4)$$

where

$$h_f = h_* + \int_{T_*}^T C_{p_f} dT$$

h_* =reference enthalpy

T_* =reference temperature

C_{p_f} =specific heat at constant pressure

The latent heat content can vary between zero (for a solid) and L (for a liquid).

For solidification/melting problems, the energy equation is written as follows:

$$\frac{\delta}{\delta t}(\rho_f H_f) + \nabla \cdot (\rho_f \vec{V}_f H_f) = \nabla \cdot (K \nabla T) + S \quad (5)$$

where

H_f =enthalpy \vec{V}_f =fluid velocity

ρ_f =density S =source term

The density result and heat capacity of PCM composites can be calculated using mixing rules. The melting fraction is the ratio of the latent heat to the total enthalpy, which was derived in the previous work investigation [17] and expressed as follows:

$$\text{melting fraction} = \frac{T - T_s}{T_l - T_s} \quad (6)$$

Conventional heat exchanger correlations are used to investigate the heat transfer properties of the systems. The speed and temperature values observed in the lab are part of the experimental data. The thermo-physical parameters of the air were measured at the average temperature of the atmosphere, or T_b .

$$T_b = \frac{T_{in} + T_{out}}{2} \quad (7)$$

where T_{in} and T_{out} represent the temperature of the air at the beginning and end of the air channels, respectively. According to Newton's rule of cooling, the ratio of heat transmission by convection, also known as thermal power (Q), between heated PCMs and cold air may be defined as follows:

It situated between the PCMs and the air. According to the analysis of the energy balance, the amount of heat transferred from the PCMs to the air, moving through the air passageways, is equivalent to the amount of energy added to the air 'neglecting the losses of heat'.

$$Q = m C_p (T_{in} - T_{out}) \quad (8)$$

where C_p is the 'specific heat' of air when it is at a constant pressure, and m is the 'mass flow rate' of air.

Then, it was used in the computation of the dimensionless number known as the Nusselt number (Nu), as follows:

$$Nu = \frac{h D}{K_a} \quad (9)$$

where K_a represents the thermal conduction of air.

To create the model mesh, we used Gambit, a software tool for geometric modelling that includes mesh generation capabilities. A tetrahedral mesh was constructed, as depicted in Figure 3. Multiple grid sizes were tested and evaluated using FLUENT software to determine the most suitable grid size for the mesh. The liquid fraction tests were conducted on each grid, and the results were compared, as shown in the table. The findings suggest that the liquid fraction measurements were consistent between mesh numbers 256443 and 325127. Therefore, the optimal mesh number for the entire process is 256443, as depicted in Figure 4.

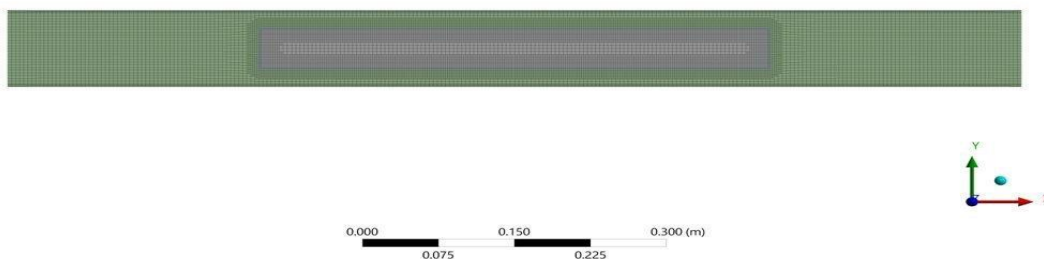


Figure (3) Mesh of the present model.

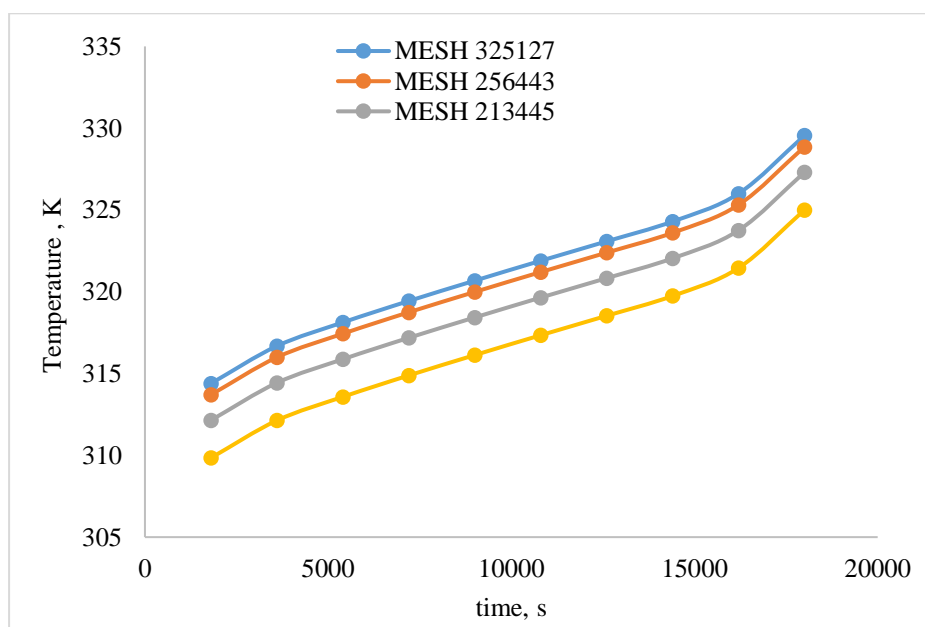


Figure (4) Mesh dependent analysis.

3. Results and Discussion

3.1 Effect of inlet velocity

The experimental study investigates the thermal storage behaviour during heat absorption through a refrigeration duct system. The results are presented in Figures 5 and 6, which illustrate the transient behaviour of heat absorption for different velocities and porous media presence/absence cases. The general trend shows that the heat transfer rate decreases over time. The presence of the porous media provides resistance to heat absorption, particularly at low velocities, resulting in a relatively slow heat release. The timing of heat transfer becomes slow as the velocity decreases, with the maximum value observed at 1.5 m/s, where the heat can be stored for up to 6000 seconds. The thermal residence time is higher at low velocities than at high velocities.

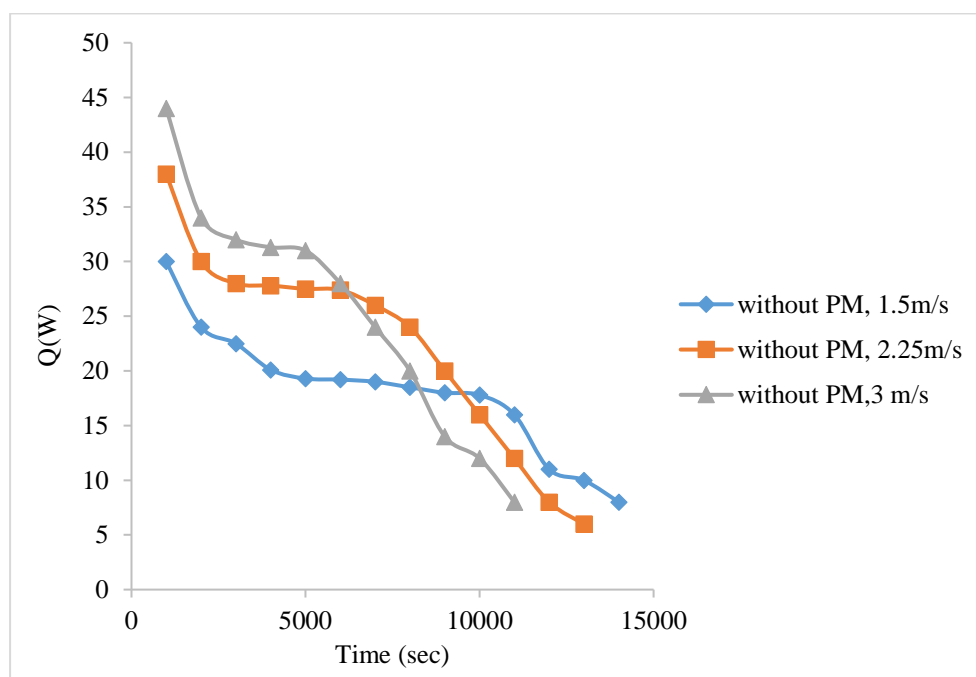


Figure 5: Transient heat absorption behaviour for various inlet velocities, without porous media case.

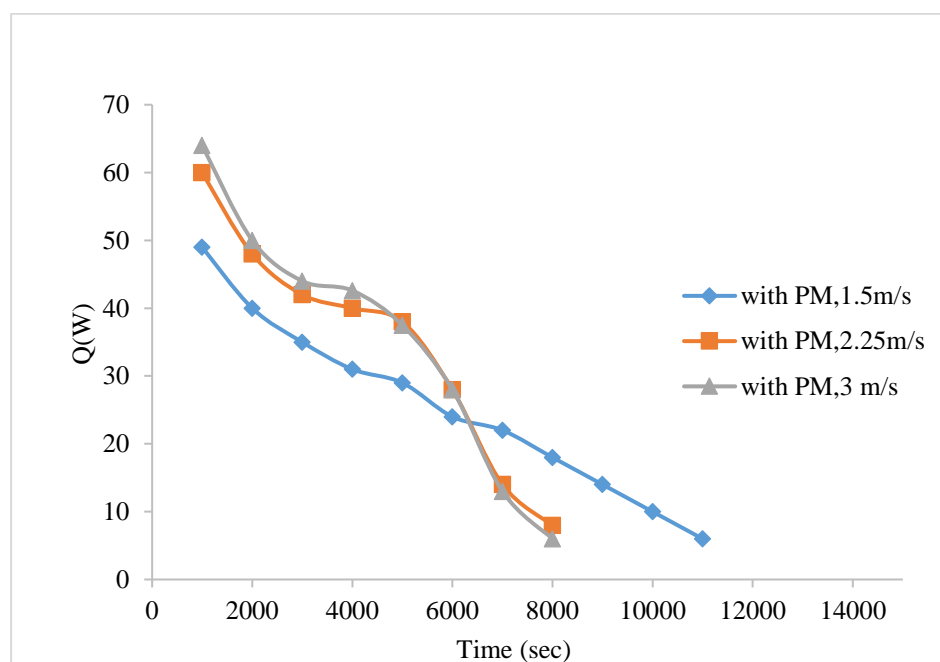


Figure 6: Transient heat absorption behaviour for various inlet velocities, with porous media case.

The study’s findings are presented in Figures 7 and 8, which display the transient behaviour of the Nusselt number under different velocities and porous media presence/absence scenarios. The Nusselt number decreases slightly over time, but it increases as the velocity increases in all cases. The maximum Nusselt number is observed at a velocity of 3 m/s. Without the porous media, the heat transfer enhancement is significantly high, reaching up to 90%, whereas it only reaches up to 25% with porous media. Increasing the velocity increases the turbulence intensity, resulting in a decrease in the thermal boundary layer’s presence.

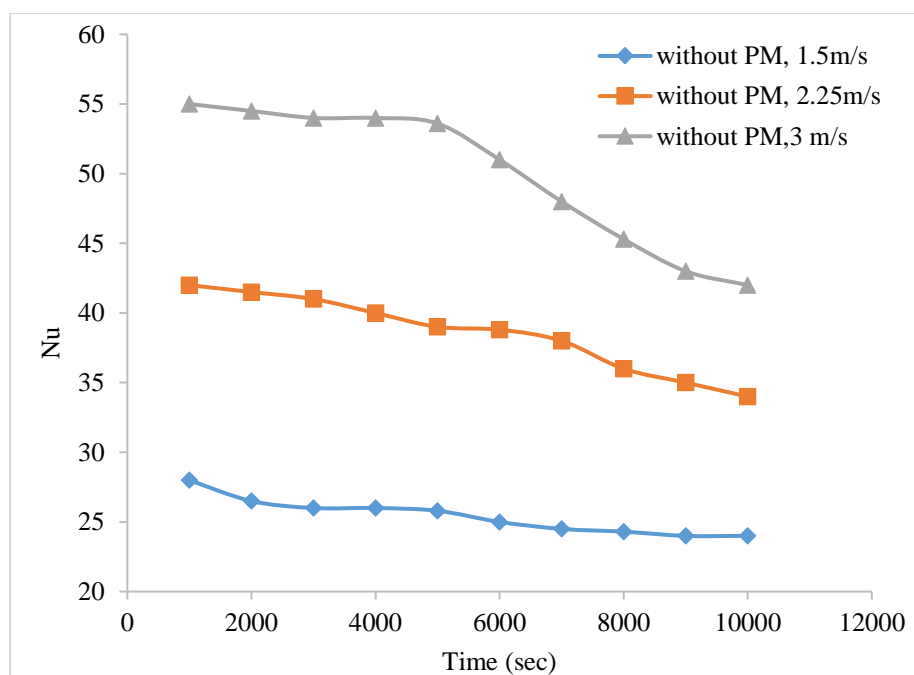


Figure 7: Transient Nu behaviour for various inlet velocities, without porous media case.

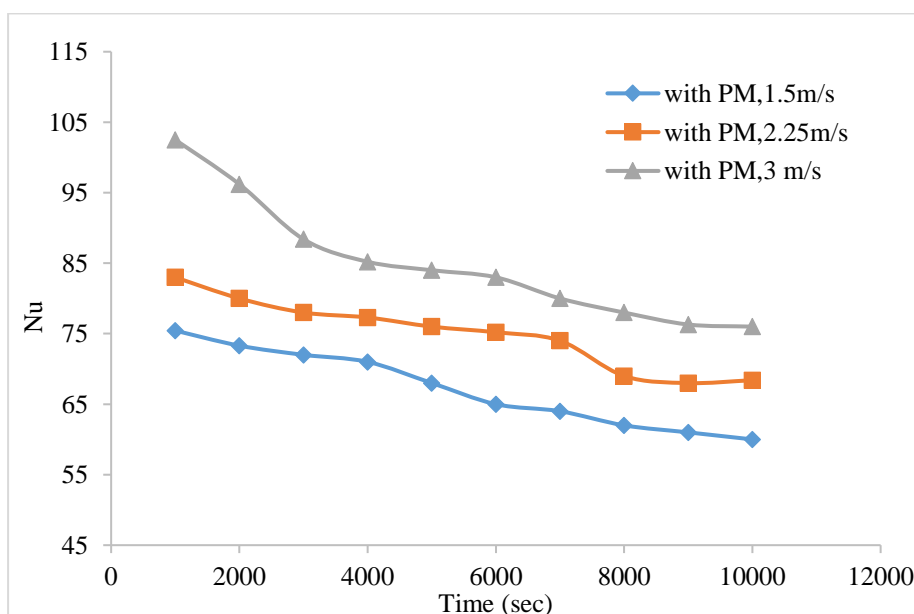


Figure 8: Transient Nu behaviour for various inlet velocities, with porous media case.

3.2 Effect of porous media

The study results are presented in Figures 9 and 10, which demonstrate the transient behaviour of the Nusselt number for with and without porous media cases at different velocities. The presence of porous media significantly enhances heat transfer, with an improvement of up to 150% at a low velocity of 1.5 m/s and 110% at an inlet velocity of 2.25 m/s. The presence of metal foam porous media enhances the heat transfer rate due to the solid–fluid interaction that increases turbulence intensity. In addition, the interfacial area surrounding the PCM capsule increases, thereby enhancing the heat transfer area.

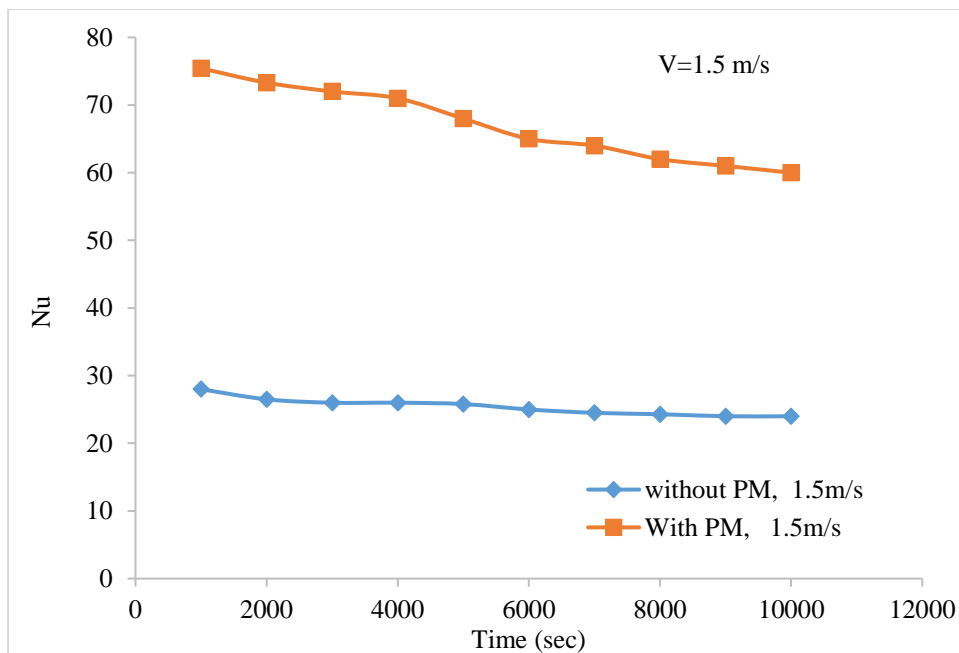


Figure 9: Comparison of Nu between porous media presence and absence (inlet velocity=1.5 m/s).

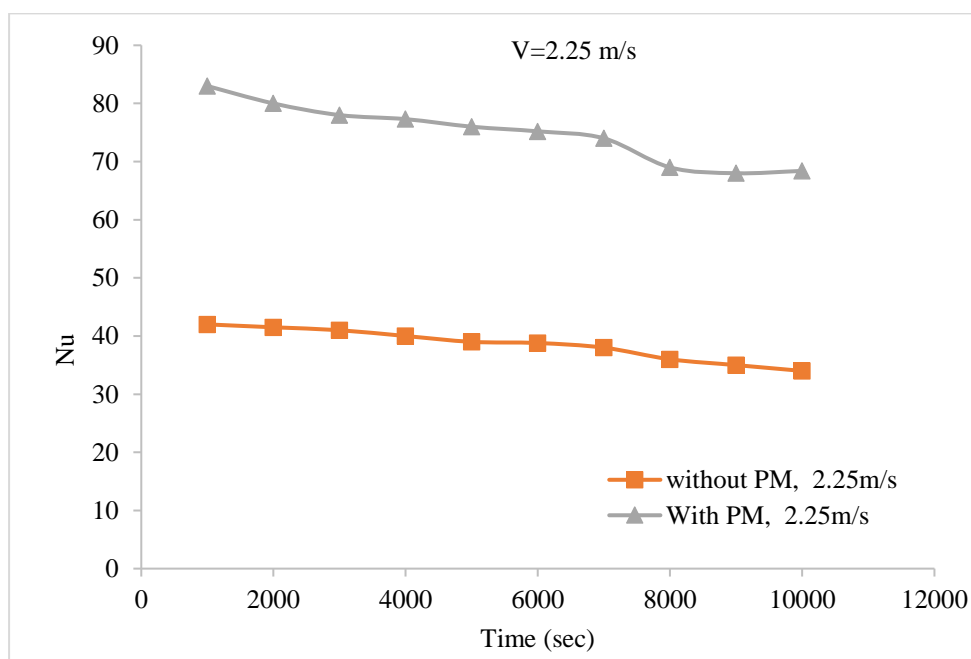


Figure 10: Comparison of Nu between porous media presence and absence (inlet velocity=2.25 m/s).

3.3 Validation

Figure 11 presents the comparison between the numerical and experimental results for various cases (with and without porous media). The validation shows good agreement between the two, with a value of 85% observed for the case without porous media and 95% for the case with porous media.

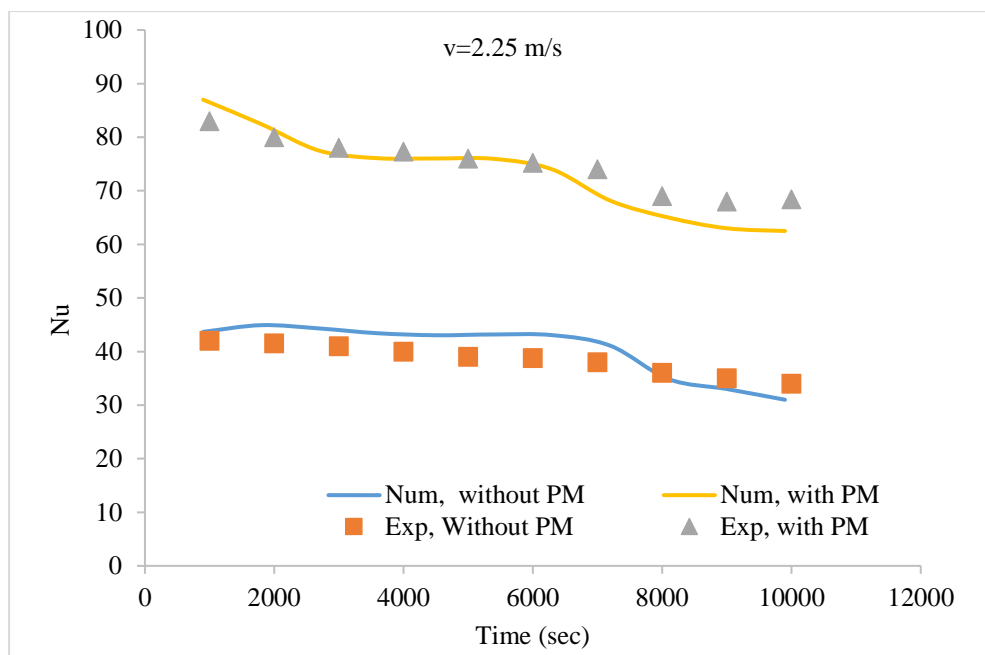
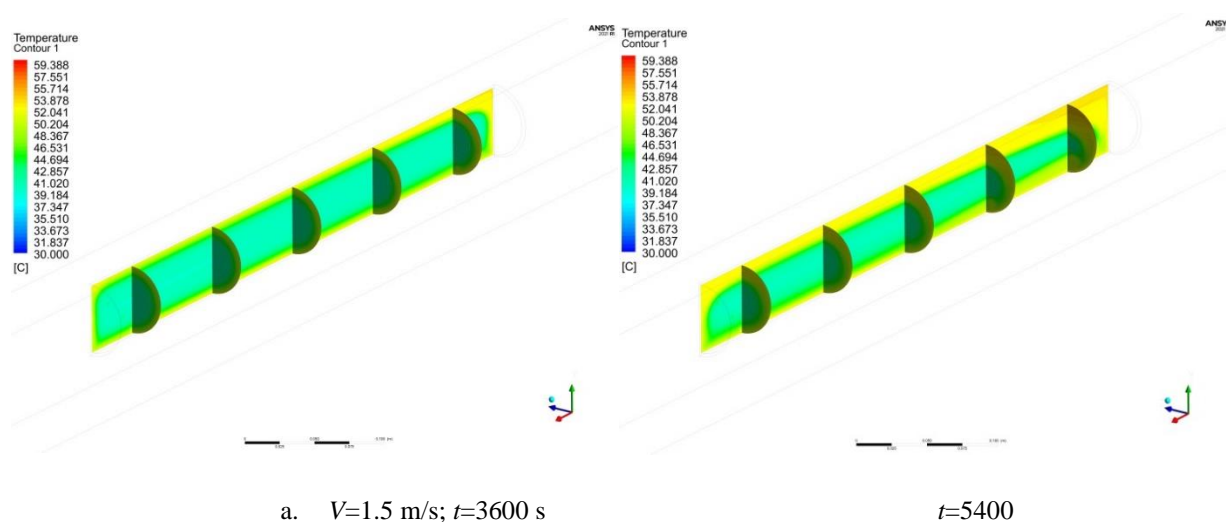


Figure 11: Validation analysis.

3.4 Contour analysis

Figure 12 displays the contour analysis of temperature distribution for different velocities and timing in the case without porous media. The analysis reveals that the general behaviour is the saturation of the PCM capsule with heat over time. As the velocity increases, the heat saturation also increases because hot gas can transfer heat more effectively at high velocities than at low velocities. This behaviour is due to the reduction of the thermal boundary layer and the increase in turbulence intensity with high velocities, enhancing the heat transfer rate. The contour analysis of temperature distribution provides a comprehensive visualisation of the heat transfer process, which is useful for understanding and optimising the design and performance of thermal storage systems.



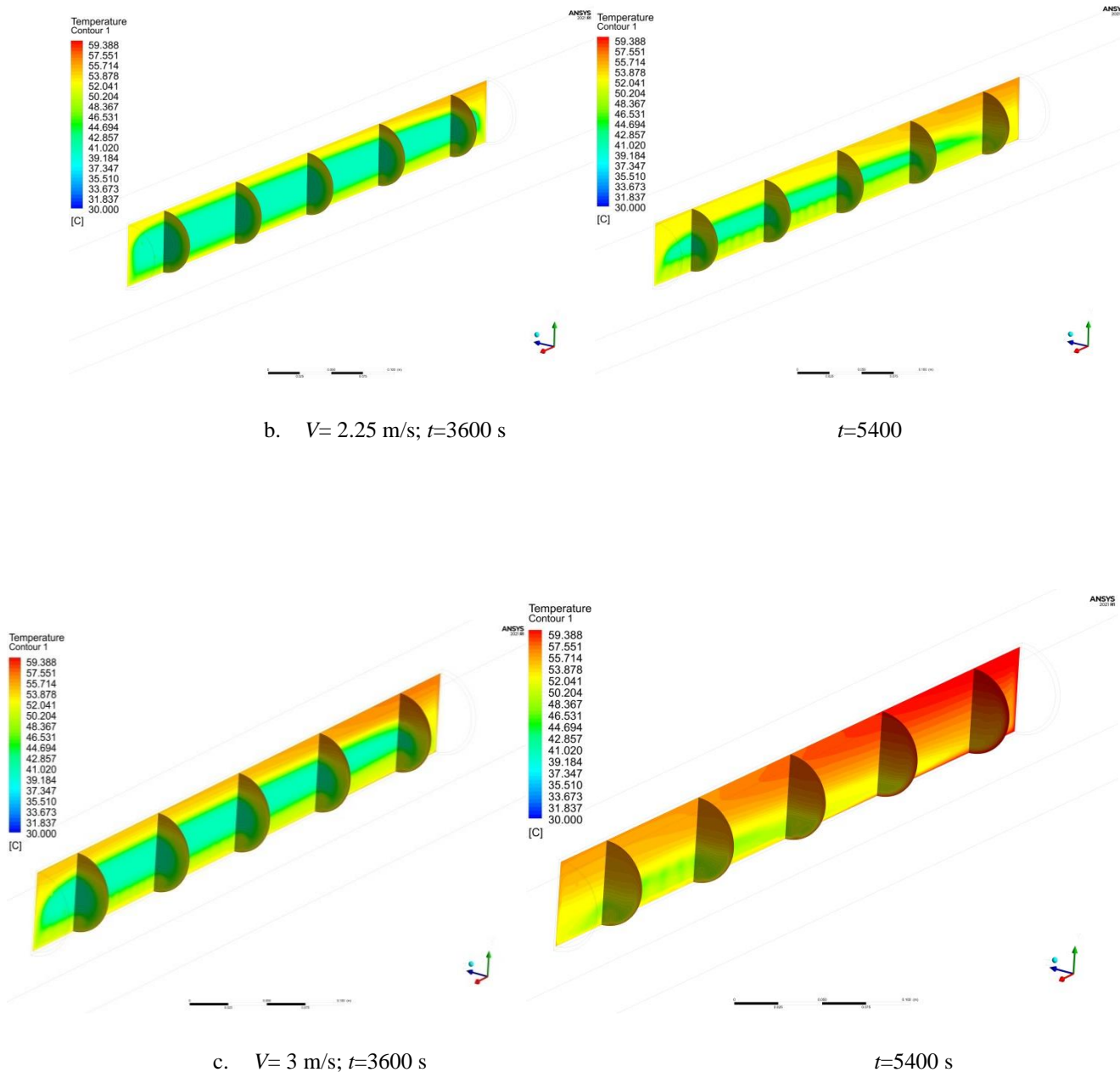


Figure 12: Contour analysis of various velocities, without porous media.

Figure 13 shows the contour analysis of temperature distribution for different cases (with and without porous media) at a velocity of 2.25 m/s. The analysis indicates that the presence of porous media significantly enhances the heat transfer rate, resulting in a more effective heat saturation than the case without porous media. This enhancement is due to the increase in turbulence intensity and interfacial area surrounding the PCM capsule, which enhances the heat transfer area. The contour analysis of temperature distribution provides a detailed insight into the heat transfer behaviour, allowing a better understanding of the thermal storage system’s design and performance, particularly with the presence of porous media.

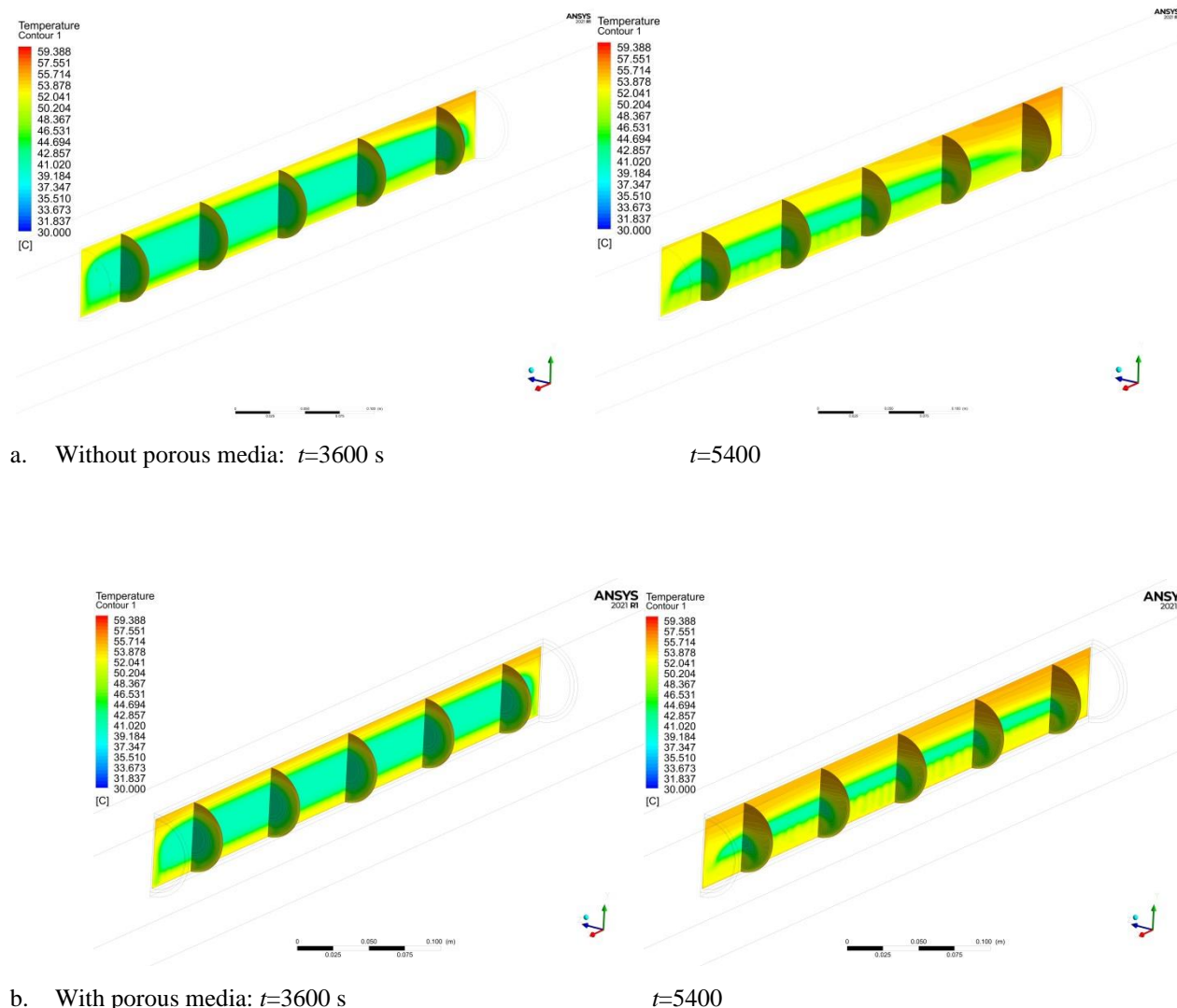


Figure 13: Contour analysis of various cases: porous media presence/absence $V=2.25$ m/s.

4. Conclusions

In summary, the experimental study investigated the thermal storage behaviour of a refrigeration duct system under different velocities and porous media presence/absence scenarios. The following conclusions are drawn:

- 1- The study results indicated that the heat transfer rate decreased over time, and the presence of porous media provided resistance to heat absorption, resulting in a slower heat release, particularly at lower velocities.
- 2- The maximum thermal residence time was observed at 1.5 m/s, where heat could be stored for up to 6000 seconds. The Nusselt number decreased slightly over time, but it increased as the velocity increased in all cases.
- 3- Without the presence of porous media, the heat transfer enhancement was significantly higher, reaching up to 90%, but with porous media, it only reached up to 25%.
- 4- The presence of porous media, such as a metal foam, significantly enhanced heat transfer, with an improvement of up to 150% at a low velocity of 1.5 m/s and 110% at an inlet velocity of 2.25 m/s.
- 5- The validation between the numerical and experimental results showed good agreement, with a value of 85% observed for the case without porous media and 95% for the case with porous media.
- 6- The contour analysis of temperature distribution provided a comprehensive visualisation of the heat transfer process, which was useful for understanding and optimising the design and performance of thermal storage systems. Overall, the findings suggest that the presence of porous media significantly enhances the heat transfer rate and the thermal storage capacity of the refrigeration duct system.
- 7- The study results could have significant implications for the development of more efficient and effective thermal storage systems for various applications, particularly in the field of refrigeration and air conditioning.

References

- [1] Wen, R., Zhang, W., Lv, Z., Huang, Z., Gao, W. (2018). A novel composite Phase change material of Stearic Acid/Carbonized sunflower straw for thermal energy storage. *Materials Letters*, 215: 42-45. <https://doi.org/10.1016/j.matlet.2017.12.008>
- [2] Papadimitratos, A., Sobhansarbandi, S., Pozdin, V., Zakhidov, A., Hassanipour, F. (2016). Evacuated tube solar collectors integrated with phase change materials. *Solar Energy*, 129: 10-19. <https://doi.org/10.1016/j.solener.2015.12.040>
- [3] Muratore, C., Aouadi, S.M., Voevodin, A.A. (2012). Embedded phase change material microinclusions for thermal control of surfaces. *Surface and Coatings Technology*, 206(23): 4828-4832. <https://doi.org/10.1016/j.surfcoat.2012.05.030>
- [4] Du, K., Calautit, J., Wang, Z., Wu, Y., Liu, H. (2018). A review of the applications of phase change materials in cooling, heating and power generation in different temperature ranges. *Applied energy*, 220: 242-273. <https://doi.org/10.1016/j.apenergy.2018.03.005>
- [5] Liu, C., Groulx, D. (2014). Experimental study of the phase change heat transfer inside a horizontal cylindrical latent heat energy storage system. *International Journal of Thermal Sciences*, 82: 100-110. <https://doi.org/10.1016/j.ijthermalsci.2014.03.014>
- [6] Zhang, N., Yuan, Y., Cao, X., Du, Y., Zhang, Z., Gui, Y. (2018). Latent heat thermal energy storage systems with solid–liquid phase change materials: a review. *Advanced Engineering Materials*, 20(6): 1700753. <https://doi.org/10.1002/a-dem.201700753>
- [7] Liu, C., Yuan, Y., Zhang, N., Cao, X., & Yang, X. (2014). A novel PCM of lauric–myristic–stearic acid/expanded graphite composite for thermal energy storage. *Materials Letters*, 120: 43-46. <https://doi.org/10.1016/j.matlet.2014.01.051>
- [8] Cabeza, L.F., Castell, A., Barreneche, C.D., De Gracia, A., Fernández, A.I. (2011). Materials used as PCM in thermal energy storage in buildings: A review. *Renewable and Sustainable Energy Reviews*, 15(3), 1675-1695. <https://doi.org/10.1016/j.rser.2010.11.018>
- [9] Regin, A.F., Solanki, S.C., Saini, J.S. (2008). Heat transfer characteristics of thermal energy storage system using PCM capsules: a review. *Renewable and Sustainable Energy Reviews*, 12(9): 2438-2458. <https://doi.org/10.1016/j.rser.2007.06.009>
- [10] Sari, A., Karaipekli, A. (2007). Thermal conductivity and latent heat thermal energy storage characteristics of paraffin/expanded graphite composite as phase change material. *Applied thermal engineering*, 27(8-9): 1271-1277. <https://doi.org/10.1016/j.applthermaleng.2006.11.004>
- [11] Akgün, M., Aydın, O., Kaygusuz, K. (2008). Thermal energy storage performance of paraffin in a novel tube-in-shell system. *Applied thermal engineering*, 28(5-6): 405-413. <https://doi.org/10.1016/j.applthermaleng.2007.05.013>
- [12] Yuan, Y., Zhang, N., Tao, W., Cao, X., He, Y. (2014). Fatty acids as phase change materials: A review. *Renewable and Sustainable Energy Reviews*, 29: 482-498. <https://doi.org/10.1016/j.rser.2013.08.107>

- [13] Agyenim, F., Eames, P., Smyth, M. (2010). Heat transfer enhancement in medium temperature thermal energy storage system using a multitube heat transfer array. *Renewable energy*, 35(1): 198-207. <https://doi.org/10.1016/j.renene.2009.03.010>
- [14] Esapour, M., Hosseini, M.J., Ranjbar, A.A., Pahamli, Y., Bahrampoury, R. (2016). Phase change in multi-tube heat exchangers. *Renewable Energy*, 85: 1017-1025. <https://doi.org/10.1016/j.renene.2015.07.063>
- [15] Liu, H., Li, S., Chen, Y., Sun, Z. (2014). The melting of phase change material in a cylinder shell with hierarchical heat sink array. *Applied thermal engineering*, 73(1): 975-983. <https://doi.org/10.1016/j.applthermaleng.2014.08.062>
- [16] Liu, J., Xu, C., Ju, X., Yang, B., Ren, Y., Du, X. (2017). Numerical investigation on the heat transfer enhancement of a latent heat thermal energy storage system with bundled tube structures. *Applied Thermal Engineering*, 112: 820-831. <https://doi.org/10.1016/j.applthermaleng.2016.10.144>
- [17] Jesumathy, S.P., Udayakumar, M., Suresh, S., Jegadheeswaran, S. (2014). An experimental study on heat transfer characteristics of paraffin wax in horizontal double pipe heat latent heat storage unit. *Journal of the Taiwan Institute of Chemical Engineers*, 45(4): 1298-1306. <https://doi.org/10.1016/j.jtice.2014.03.007>
- [18] Kousha, N., Rahimi, M., Pakrouh, R., Bahrampoury, R. (2019). Experimental investigation of phase change in a multitube heat exchanger. *Journal of Energy Storage*, 23: 292-304. <https://doi.org/10.1016/j.est.2019.03.024>
- [19] Joybari, M.M., Seddegh, S., Wang, X., Haghghat, F. (2019). Experimental investigation of multiple tube heat transfer enhancement in a vertical cylindrical latent heat thermal energy storage system. *Renewable Energy*, 140: 234-244. <https://doi.org/10.1016/j.renene.2019.03.037>
- [20] Alizadeh, M., Pahlavanian, M.H., Tohidi, M., Ganji, D. D. (2020). Solidification expedition of Phase Change Material in a triplex-tube storage unit via novel fins and SWCNT nanoparticles. *Journal of Energy Storage*, 28: 101188. <https://doi.org/10.1016/j.est.2019.101188>
- [21] Yuan, Y., Cao, X., Xiang, B., Du, Y. (2016). Effect of installation angle of fins on melting characteristics of annular unit for latent heat thermal energy storage. *Solar energy*, 136: 365-378. <https://doi.org/10.1016/j.solener.2016.07.014>
- [22] Mosaffa, A.H., Talati, F., Tabrizi, H.B., Rosen, M.A. (2012). Analytical modeling of PCM solidification in a shell and tube finned thermal storage for air conditioning systems. *Energy and buildings*, 49: 356-361. <https://doi.org/10.1016/j.enbuild.2012.02.053>
- [23] Baby, R., Balaji, C. (2013). Thermal optimization of PCM based pin fin heat sinks: an experimental study. *Applied Thermal Engineering*, 54(1): 65-77. <https://doi.org/10.1016/j.applthermaleng.2012.10.056>
- [24] Yousef, M.S., Hassan, H., Kodama, S., Sekiguchi, H. (2019). An experimental study on the performance of single slope solar still integrated with a PCM-based pin-finned heat sink. *Energy Procedia*, 156: 100-104. <https://doi.org/10.1016/j.egypro.2018.11.102>
- [25] Sun, Z., Fan, R., Yan, F., Zhou, T., Zheng, N. (2019). Thermal management of the lithium-ion battery by the composite PCM-Fin structures. *International Journal of Heat and Mass Transfer*, 145: 118739. <https://doi.org/10.1016/j.ijheatmasstransfer.2019.118739>
- [26] Acir, A., Canli, M.E. (2018). Investigation of fin application effects on melting time in a latent thermal energy storage system with phase change material (PCM). *Applied Thermal Engineering*, 144: 1071-1080. <https://doi.org/10.1016/j.applthermaleng.2018.09.013>

- [27] Sciacovelli, A., Gagliardi, F., Verda, V. (2015). Maximization of performance of a PCM latent heat storage system with innovative fins. *Applied Energy*, 137: 707-715. <https://doi.org/10.1016/j.apenergy.2014.07.015>
- [28] Mat, S., Al-Abidi, A.A., Sopian, K., Sulaiman, M.Y., Mohammad, A.T. (2013). Enhance heat transfer for PCM melting in triplex tube with internal-external fins. *Energy conversion and management*, 74: 223-236. <https://doi.org/10.1016/j.enconman.2013.05.003>
- [29] Khan, Z., Khan, Z., Tabeshf, K. (2016). Parametric investigations to enhance thermal performance of paraffin through a novel geometrical configuration of shell and tube latent thermal storage system. *Energy Conversion and Management*, 127: 355-365. <https://doi.org/10.1016/j.enconman.2016.09.030>
- [30] Yang, X., Lu, Z., Bai, Q., Zhang, Q., Jin, L., Yan, J. (2017). Thermal performance of a shell-and-tube latent heat thermal energy storage unit: Role of annular fins. *Applied energy*, 202: 558-570. <https://doi.org/10.1016/j.apenergy.2017.05.007>
- [31] Wang, P., Yao, H., Lan, Z., Peng, Z., Huang, Y., Ding, Y. (2016). Numerical investigation of PCM melting process in sleeve tube with internal fins. *Energy Conversion and Management*, 110: 428-435. <https://doi.org/10.1016/j.enconman.2015.12.042>.
- [32] Khodabandeh, E., Dastjerdi, M. S., Shokri, M., & Akhavan-Behabadi, M. A. (2020). Experimental investigation of paraffin wax as a phase change material in a domestic refrigerator. *Applied Thermal Engineering*, 173, 115214.
- [33] Wang, F., Zheng, X., Wu, J., & Zhou, D. (2020). Experimental investigation of a refrigeration system with capric-lauric acid eutectic mixture as a phase change material. *Applied Thermal Engineering*, 177, 115350.
- [34] Zhang, Y., Zhang, B., & Wu, J. (2019). A novel refrigeration system with phase change materials based thermal storage unit. *Energy Conversion and Management*, 180, 72-82.
- [35] Zhu, X., Liu, W., Liu, G., Zhang, Y., & Wang, R. (2019). A novel hybrid refrigeration system using phase change materials as thermal storage. *Applied Energy*, 241, 257-270.
- [36] Zhang, Y., Li, Y., & Wu, J. (2018). Application of phase change material-based thermal storage unit in supermarket refrigeration systems. *Applied Energy*, 210, 644-655.